



Revealing the intrinsic mechanisms for accelerating nitrogen removal efficiency in the Anammox reactor by adding Fe(II) at low temperature

Linjing Li^a, Wenlai Xu^a, Jianyong Ning^a, Yaping Zhong^{c,f}, Chuyue Zhang^{d,e}, Jiane Zuo^{b,g}, Zhicheng Pan^{b,c,e,*}

^a State Key Laboratory of Geohazard Prevention and Geoenvironment Protection, Chengdu University of Technology, Chengdu 610059, China

^b State Key Joint Laboratory of Environment Simulation and Pollution Control, School of Environment, Tsinghua University, Beijing 100084, China

^c National Postdoctoral Research Station, Haitian Water Group, Chengdu 610213, China

^d National Enterprise Technology Center, Haitian Water Group, Chengdu 610213, China

^e Water Safety and Water Pollution Control Engineering Technology Research Center in Sichuan Province, Chengdu 610213, China

^f Laboratory of Municipal Wastewater Treatment Technology in Sichuan Province, Chengdu 610213, China

^g Institute of Environment and Ecology, Tsinghua Shenzhen International Graduate School, Shenzhen 518055, China

ARTICLE INFO

Article history:

Received 8 August 2023

Revised 29 August 2023

Accepted 23 October 2023

Available online 2 November 2023

Keywords:

Ambient low temperature

Anammox

Fe(II)

Extracellular polymeric substances

Microbial community

Microbial network analysis

ABSTRACT

Fe(II) is an essential trace element for anaerobic ammonium oxidation bacteria (AAOB) metabolism, and can improve the nitrogen removal efficiency of anaerobic ammonia oxidation (Anammox). Here we operated two identical expanded granular sludge bed (EGSB) reactors at low temperature (15 ± 3 °C) for 154 days. Reactor 1 (R_1) received additional Fe(II) (0.12 mmol/L) during the late startup phase, while reactor 0 (R_0) served as the control and did not receive extra Fe(II). Nitrogen removal in R_1 became stable at 55 d of operation, ten days earlier than R_0 . The nitrogen removal rate (NRR) of R_1 was $1.64 \text{ kg N m}^{-3} \text{ d}^{-1}$ and its TN removal rate was as high as 89%, while R_0 only reached 75%. The addition of Fe(II) was further beneficial to aggregation and stability of the granular sludge, and the used sludge of both reactors showed enrichment for AAOB populations compared to the inoculum, for instance, increased abundance of *Candidatus-Kuenenia* and in particular of *Candidatus-Brocadia* (from 0.17% to 10.10% in R_0 and 7.79% in R_1). Diverse microbial species and complex microbial network structure in R_1 compared to R_0 promoted the coupled denitrogenation by Anammox, dissimilatory nitrate reduction to ammonium (DNRA), nitrate-dependent Fe oxidation (NDFO), and ferric ammonium oxidation (Feammox). In addition, the microbial community in R_1 was more resistant to short-term low temperature (2–7 °C) starvation, illustrating a further positive effect of adding Fe(II) during the startup phase of an Anammox reactor.

© 2024 Published by Elsevier B.V. on behalf of Chinese Chemical Society and Institute of Materia Medica, Chinese Academy of Medical Sciences.

Anaerobic ammonia oxidation (Anammox) is a new type of nitrogen removal process that uses NO_2^- as electron acceptor and NH_4^+ as electron donor under anaerobic conditions [1]. The advantages of Anammox are the independence of an external organic carbon source [2], and low production of greenhouse gasses and sludge [3]. Therefore, its application for nitrogen removal from wastewater has become a current research hotspot. However, several challenges remain to be solved, such as the slow growth of anaerobic ammonia oxidizing bacteria (AAOB) and their susceptibility to environmental disturbances [4], as these hinder the broad application of Anammox for water treatment.

Low-temperature conditions can limit the growth of AAOB. In most cases, the average temperature of actual wastewater is below 20 °C [5,6], while the optimum temperature for AAOB growth is 35–40 °C [7]. When the ambient temperature is not within the optimal temperature range, this limits the nitrogen removal performance of Anammox, as it negatively affects enzyme activity and reaction activation energy as well as bacterial growth. For instance, a decrease in water temperature from 30 °C to 15 °C resulted in a specific anaerobic ammonia oxidation activity (SAA) from $850 \text{ mg g}^{-1} \text{ d}^{-1}$ to $47 \text{ mg g}^{-1} \text{ d}^{-1}$ [8], and the growth rate of AAOB decreased by 30%–40% for every 5 °C decrease in temperature [9]. From the perspective of energy saving and consumption reduction, ambient temperature denitrogenation would be optimal for future wastewater treatment. However, even though studies have confirmed that Anammox can be started up and operated at low temperatures [10], under

* Corresponding author at: State Key Joint Laboratory of Environment Simulation and Pollution Control, School of Environment, Tsinghua University, Beijing 100084, China.

E-mail address: panzc18@mails.tsinghua.edu.cn (Z. Pan).

those conditions the process suffers from long startup times, unstable nitrogen removal efficiency, and low functional microbial abundance.

Fe(II) is an essential trace element for AAOB metabolism, and as part of the cofactor heme c, it participates in the electron transfer process in cellular metabolism [4], which in turn improves Anammox metabolic performance. The addition of Fe(II) to an Anammox system couples other denitrogenation reactions in the system and improves the denitrogenation efficiency. Ding *et al.* showed that in the presence of 0.12 mmol/L Fe(II) the Anammox activity was optimal and this stimulated microbial proliferation [11]. Qiao *et al.* reported a 30% Anammox nitrogen removal efficiency increase when Fe(II) concentrations were raised from 0.03 mmol/L to 0.09–0.12 mmol/L [12]. However, these studies had determined the optimal Fe(II) concentration at a temperature between 30 °C and 35 °C, while the required concentration at lower temperatures remains to be determined, and the mechanism of action of Anammox mediated by additional Fe(II) under such conditions is lacking. Therefore, in order to promote the large-scale application of Anammox in practical wastewater treatment, we conducted a study to investigate the mechanism of Fe(II)-mediated nitrogen removal by Anammox at a temperature of 15 ± 3 °C.

Two identical experimental expanded granular sludge bed (EGSB) reactors were used to compare the effect of extra added Fe(II) during the startup phase. The changes of water quality and granular sludge properties in the two reactors were recorded to determine: (1) The long-term effects of Fe(II) addition to an Anammox system at ambient low temperature; (2) The internal structures of the extracellular polymeric substances (EPS) that were formed; (3) The microbial community that formed during Anammox operation, in order to provide a theoretical basis and realistic reference for further application of Anammox in practical wastewater treatment.

On the first day after sludge inoculation, the $\text{NH}_4^+\text{-N}$ removal rate of R_0 and R_1 was only 9% and 64%, respectively, while the $\text{NO}_2^-\text{-N}$ removal rate was more than 96%. The large difference in $\text{NH}_4^+\text{-N}$ removal between the two reactors may be due to an uneven inoculation of the initial sludge, which leads to the difference in sludge adaptation to the reactor; and the difference in influent water conditions between the two reactors, such as dissolved oxygen content. The accumulation of $\text{NO}_3^-\text{-N}$ as an Anammox product is negative, and the ratio of $\text{NO}_3^-\text{-N}/\text{NH}_4^+\text{-N}$ was higher than the theoretical value of 1.32 for both reactors and while the $\text{NO}_3^-\text{-N}/\text{NH}_4^+\text{-N}$ ratio was less than 0 and thus lower than the theoretical value of 0.26 (Fig. 1) [13]. This indicated that the system did not produce or consume the generated $\text{NO}_3^-\text{-N}$, the intrinsic reason the initial lysis of microbes had taken place, due to the sudden changes in environmental conditions, which released organic carbon that promoted the proliferation of heterotrophic denitrifying bacteria [14]. Thus, the nitrogen removal process was initially dominated by denitrification reactions. The $\text{NH}_4^+\text{-N}$ removal rates in both reactors increased rapidly, to reach 98% and 99% on 6 d, while the $\text{NO}_2^-\text{-N}$ removal rate remained at a high level, above 96%. The high efficiency of $\text{NH}_4^+\text{-N}$ removal during this short time was attributed to two possible effects: an increase of AAOB activity, and the incomplete removal of dissolved oxygen from the influent water, resulting in nitrification. On 12 d, the influent nitrogen load rate (NLR) was increased to $0.68 \text{ kg N m}^{-3} \text{ d}^{-1}$ (Table S1 in Supporting information). Now the $\text{NH}_4^+\text{-N}$ removal rates of both reactors fluctuate dramatically (R_0 between 43% and 77%, R_1 between 34% and 61%). The $\text{NO}_2^-\text{-N}$ removal rates were now very low: in R_0 it decreased from 99% to 43% and in R_1 from 96% to 34%. This indicated an inability of AAOB to adapt to the dramatic increase of NLR in the initial stage. Therefore, the NLR decreased to $0.58 \text{ kg N m}^{-3} \text{ d}^{-1}$, and as a result the nitrogen removal efficiency of both reactors gradually improved.

Unexpectedly, on 38 d, the water bath heating system broke and the temperature plummeted to 5 °C, decreasing the nitrogen removal performance of both reactors dramatically, to removal rates of 62% for $\text{NH}_4^+\text{-N}$ and 26% $\text{NO}_2^-\text{-N}$ in R_0 , and 62% and 50%, respectively, in R_1 . That a sudden decrease in temperature having such strong impacts has been observed before [8].

After repairing the water bath heating unit, the effect of daily Fe(II) addition at a concentration of 0.12 mmol/L was tested in R_1 , which was performed from 39 d to 85 d and from 100 d to 154 d, R_0 served as the control. By 53 d, the $\text{NH}_4^+\text{-N}$ removal rate had increased to over 95% in both reactors, and the $\text{NO}_2^-\text{-N}$ removal rate had increased (R_0 : 52%, R_1 : 74%). The stoichiometric ratio $\text{NO}_2^-\text{-N}/\text{NH}_4^+\text{-N}$ of R_1 was now close to the theoretical value of 1.32, while for R_0 it remained between 0.5 to 1. It seemed that during this period, the addition of Fe(II) had a strong positive effect on the Anammox reaction for nitrogen removal. On 55 d, the NLR elevated to $0.75 \text{ kg N m}^{-3} \text{ d}^{-1}$ and that caused the $\text{NH}_4^+\text{-N}$ removal rate of both reactors to reach over 97% after acclimation, but the $\text{NO}_2^-\text{-N}$ removal rate of R_1 remained consistently higher than that of R_0 (R_0 : 70%–86%, R_1 : 82%–97%). It has been shown that AAOB can reduce $\text{NO}_3^-\text{-N}$ and $\text{NO}_2^-\text{-N}$ to N_2 , N_2O , and $\text{NH}_4^+\text{-N}$, during which Fe(II) acts as an electron donor for the dissimilatory nitrate to ammonium (DNRA) [15]. Therefore, the addition of Fe(II) may promote the coupling of denitrification, DNRA, and Anammox within the system, which would explain the higher nitrogen removal efficiency of R_1 compared to R_0 .

A nitrogen removal rate (NRR) of $0.5 \text{ kg N m}^{-3} \text{ d}^{-1}$ typically marks the successful start-up of an Anammox system [16], and according to Fig. 1, this was reached on 55 d for R_1 (NRR: $0.54 \text{ kg N m}^{-3} \text{ d}^{-1}$) but only on 65 d for R_0 (NRR: $0.53 \text{ kg N m}^{-3} \text{ d}^{-1}$), indicating that at low temperatures, the Fe(II)-added reactor was able to reduce the start-up time by 10 days compared to a blank reactor.

Before investigating the stable performance of Anammox after successful start-up, the two reactors were left idle for 13 days (86–100 d) at low temperature (2–7 °C) and on 100 d, operation of both reactors was restarted at 15 ± 3 °C with an influent of 100 mg/L $\text{NH}_4^+\text{-N}$, after which the NLR was gradually increased from $0.95 \text{ kg N m}^{-3} \text{ d}^{-1}$ to $1.75 \text{ kg N m}^{-3} \text{ d}^{-1}$. The performance of both reactors was now stable: the $\text{NH}_4^+\text{-N}$ removal rate was maintained at high levels, above 80% for R_0 and above 92% for R_1 , and the $\text{NO}_2^-\text{-N}$ removal rate was 79% for R_0 and 90% for R_1 . These results showed that the bacterial communities were able to maintain good nitrogen removal performance even after short-term starvation conditions, and since they were adapted to low temperature (15 ± 3 °C), a cold starvation period at 2–7 °C did not have a large impact on their performance. It has been shown that within an Anammox system with Fe(II) addition, $\text{NH}_4^+\text{-N}$ is most likely removed by iron-ammonia oxidation (Feammox) [17]. In our experiment, nitrogen removal performance and operational stability of R_1 were superior to R_0 throughout operation (Fig. 1), indicating that the addition of moderate amounts of Fe(II) had promoted the efficient and stable operation of the Anammox system at ambient low temperatures (15 ± 3 °C).

The EPS content of the sludge samples collected over time was determined. During operation, the EPS content increased from 5 to 93 mg/g VSS in R_0 and to 136 mg/g VSS in R_1 . The EPS content of R_1 was higher than that of R_0 from 67 d onwards (Fig. 2a). Since Fe(II) is reductive, it can provide electrons during ammonia oxidation and it participates in the synthesis of related denitrogenation proteins as well. Both will improve the performance of AAOB, which in turn stimulates the AAOB community to secrete more EPS [2]. This may explain why the addition of Fe(II) in R_1 led to higher EPS content from 67 d onwards. In addition, EPS contains many anionic functional groups, leading to a preference for EPS to combine with positively charged Fe(II) and thus forming a

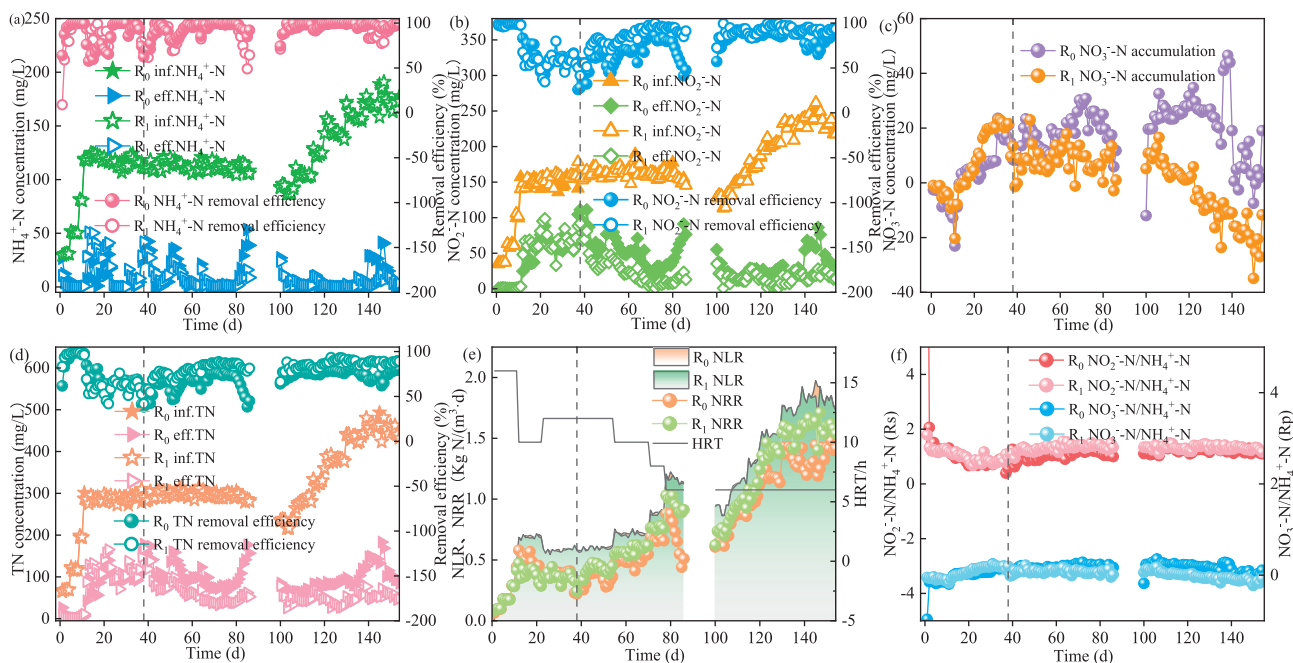


Fig. 1. Performance of both reactors, R₀ and R₁, during operation at 15 ± 3 °C. (a) ammonium nitrogen removal performance, (b) NO₂⁻-N removal performance, (c) NO₃⁻-N accumulation, (d) total nitrogen (TN) removal performance, (e) nitrogen loading rate (NLR), nitrogen removal rate (NRR) and HRT during operation over time, (f) stoichiometric ratios NO₂⁻-N/NH₄⁺-N (R_s), and NO₃⁻-N/NH₄⁺-N (R_p) for both reactors.

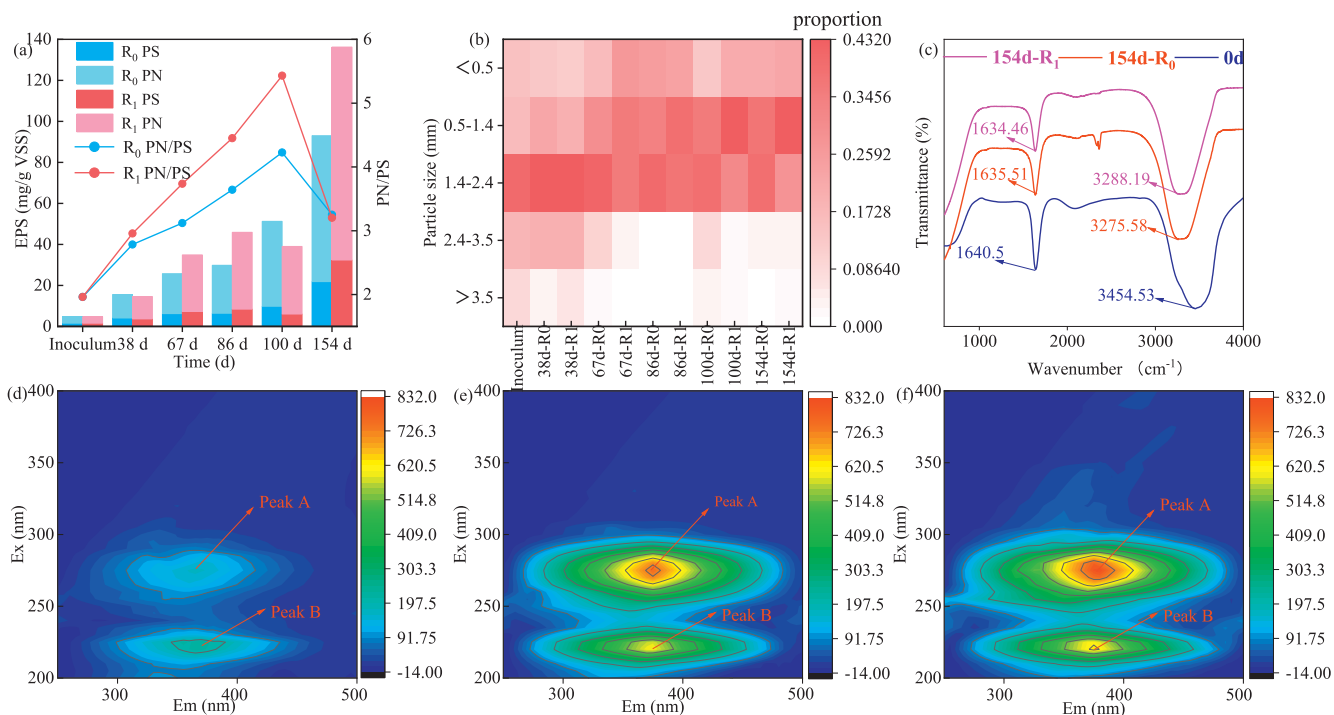


Fig. 2. (a) EPS content of the sludge samples and its protein (PN), polysaccharide (PS) fractions, (b) particle size distribution during initiation, (c) EPS fourier transform infrared (FTIR) spectra (500–4000 cm⁻¹) of the sludge used as the inoculum and after 154 d of operation in R₀ and R₁. Three-dimensional fluorescence spectra with (d) inoculum, (e) R₀ sludge at 154 d and (f) R₁ sludge at 154 d.

more stable structure to maintain the stability of granular sludge. After cold starvation, at 100 d the EPS content of R₀ had increased, while that of R₁ decreased, probably because Fe(II) had not only promoted the growth of AAOB but had also increased the abundance of other heterotrophic bacteria in the system [18]. These metabolized endogenous organic carbon sources and EPS, resulting in a slight decrease in EPS content after starvation in R₁. Xing *et al.*

reported that 4 °C starvation was more conducive to maintaining granular sludge properties [19], and our findings provide a further reference for storing sludge at low temperatures.

The fractions of the key components protein (PN) and polysaccharides (PS) of the EPS are also shown in Fig. 2a. The dominance of PN in EPS at the different time points, and the low PS content with minor variation, implies that PN plays a major role in the

properties of granular sludge. Since PN contains positively charged amino acid groups and PS is mainly negatively charged due to phosphate groups, the PN/PS ratio determines the hydrophobic properties of granular sludge [20,21]. This ratio ranged from 0.5 to 5, with lowest values at 0 d and highest values at 100 d (Fig. 2a). The higher this ratio, the more hydrophobic the EPS is, resulting in higher stability of granular sludge, thus, the hydrophobicity of the granular sludge increased with operation time and was higher following Fe(II) addition. In particular, for R_1 PN/PS exceeded 5 at 100 d following low temperature starvation, and as the system was re-operated, the ratio decreased again, but at the end of operation it was still higher than that of the inoculum.

The PN/PS ratio is related to the particle size of the sludge. Thus, the particle size distribution was determined and summarized in Fig. 2b. The inoculum mainly contained particles <3.5 mm. The main particle size of the sludge at 154 d had increased to 0.5–1.4 mm (which comprised 37% of R_0 and 42% of R_1). It has been reported that sludge with a particle size exceeding 2.2 mm is at risk of floating [22]. Chen *et al.* compared different particle sizes and SAA of Anammox sludge and found that the highest SAA content was found for particle sizes ranging from 0.5 mm to 1 mm [23]. That optimal size was applied to the granular sludge cultured in this study. This, to some extent, also explains why both reactors were able to achieve efficient and stable denitrogenation.

Functional groups present in the EPS of the inoculum and the sludge after 154 d of operation were characterized by FTIR analysis. As shown in Fig. 2c, the functional groups in EPS of all samples were similar, indicating that no changes had been introduced as a result of the cultivation in the absence or presence of additional Fe(II). The absorption peaks of 3275–3454 cm^{-1} were caused by N–H and O–H stretching vibrations in PN and PS [24] and the absorption peaks visible at 1634–1640 cm^{-1} are caused by C=O and C=C stretching vibrations in PN [25]. There were few hydrophilic functional groups in the EPS and N–H, O–H and C=O seem to be the main functional groups that promote microbial aggregation [26].

The 1600–1700 cm^{-1} wavelength range represents region I of the spectrum where the secondary structures of the protein are detected [25]. The investigated granular sludge contained β -sheets, random coils, α -helices, and β -turns (Fig. S4 in Supporting information). Their distribution varied, and in the used sludge β -sheets were dominant, representing 48.34% in inoculated sludge, 39.59% in R_0 , and 38.78% in R_1 (Table S3 in Supporting information). These β -sheets provide the Anammox sludge with a strong aggregation capacity [27]. The abundance ratio of α -helix/(β -sheet + random coil) is a measure of the tightness of the protein structure [28]. This ratio was lower in the final sludge of R_0 and R_1 compared to the inoculum, and it was lower in R_1 than in R_0 (Table S3). From this we conclude that the hydrophobic groups inside the EPS protein became more exposed over time, increasing the hydrophobicity of the granular sludge surface. This explained the hydrophobicity and aggregation characteristics of the granular sludge.

The three-dimensional fluorescence spectra of EPS of the inoculum and the used sludge at 154 d from R_0 and R_1 were measured (Figs. 2d–f). Table S4 (Supporting information) summarizes the parameters of the obtained spectra. Two peaks were identified: peak A (274–275 nm/365–377 nm) representing humic acid-like substances and peak B (220–222 nm/366–375 nm) representing tryptophan [29]. The fluorescence intensity of both peaks increased during the operation of the reactors. Independent studies have shown that the relative content of humic acid-like substances is positively correlated with bacterial activity [30], from which it is inferred that the microbial activity of the Anammox organisms was strengthened during operation. Tryptophan-like substances also increased, and these represent key substances that trigger granular sludge aggregation [31]; it also provides tolerance to high nitrogen-

containing substances [32]. Du *et al.* reported that an elevated NLR in a reactor containing PD/A granular sludge resulted in more secretion of tryptophan, increasing granular sludge stability [32], further confirming that granular sludge tends to stabilize during operation. We observed a higher fluorescence intensity for both peaks in R_1 compared to R_0 , suggesting that complexation of Fe(II) had occurred with the functional groups in EPS that increased the fluorescence intensity, while its presence had resulted in a subsequent increase of AAOB metabolites, as a result of simulated metabolic activity.

The obtained sequences were attributed to OTUs and these were assigned to genera and phyla. At the phylum level, the inoculum was dominated by Chloroflexi, Bacteroidota, Halobacterota, and Euryarchaeota (in descending order), while Planctomycetota only represented 5.52% (Fig. 3a). At the end of the operation, the abundance of Planctomycetota had strongly increased, to 17.43% (R_0) and 13.77% (R_1), together with an increase of Proteobacteria (from 10.29% in the inoculum to 18.67% in R_0 and 27.68% in R_1), while the fraction of Euryarchaeota had severely decreased. The Bacteroidota had more strongly decreased in R_0 than in R_1 (R_0 : 12.80%, R_1 : 18.18%) and in R_1 the fraction of Halobacterota had strongly decreased. The abundance of Chloroflexi remained similar (R_0 : 23.50%, R_1 : 22.96%). AAOB are mainly members of Planctomycetota [33], while Chloroflexi, Proteobacteria, and Bacteroidota are typical companion flora of AAOB [32,34,35]. Proteobacteria are mainly involved in nitrogen removal by denitrification [36]; they also secrete fibrates and soluble microbial products (SMP) that regulate the microbial diversity of a community [37], and their increase during operation implied that AAOB participated in the removal of nitrogen together with denitrifying bacteria. During operation, the abundance of Chloroflexi was maintained at around 23%, and these bacteria may be responsible for the decomposition of dead cells; they also assist in sludge granulation [38], and their high abundance ensured the stability of the sludge granules. Decreases in the archaeal phyla Halobacterota and Euryarchaeota indicated that some of these anaerobic heterotrophic bacteria were unsuitable to survive in the environment inside the reactor.

The relative abundance of the 20 most abundant microbial genera present in the three sludge samples was visualized in a heatmap (Fig. 3b). this included the AAOB genera *Candidatus_Kuenenia*, *Candidatus_Brocadia*, and *Candidatus_Jettenia*, of which *Candidatus_Brocadia* had most strongly increased (from 0.17% to 10.10% in R_0 and 7.79% in R_1). *Candidatus_Kuenenia* had also increased (from 2.78% to 5.63% in R_0 and 4.63% in R_1), but *Candidatus_Jettenia* had decreased during operation (from 1.73% to 0.67% and 0.79%, respectively). It has been shown that *Candidatus_Brocadia* is better adapted to a low-temperature environment and is more resistant to a high nitrogen load shock compared to *Candidatus_Kuenenia* or *Candidatus_Jettenia* [39–41], so the high NLR (1.7 $\text{kg N m}^{-3} \text{d}^{-1}$) and low temperature employed during operation may have caused the observed shifts in abundance. Li *et al.* reported a shift from *Candidatus_Jettenia* to *Candidatus_Brocadia* when the temperature of a reactor was reduced from 32 °C to 22 °C [42]. Wang *et al.* reported that Fe(II) can stimulate the Feamox reaction performed by *Candidatus_Brocadia* [43], and this may have increased the removal of $\text{NH}_4^+\text{-N}$ from R_1 , although this genus was more abundant in R_0 . In addition, the surface of *Candidatus_Brocadia* is rich in hydrophobic groups [44], increasing the granular sludge aggregation capacity.

Methanosaeta and *Methanobacterium* use organic carbon sources to produce CH_4 [45], and their abundance decreased during operation, resulting in lower abundance in R_1 than in R_0 . As most of the heterotrophic microorganisms that were not adapted to the environment gradually died out, the organic carbon source available to methanogenic bacteria was reduced, explaining their decrease. The denitrifying bacteria also competed with methanogenic bacteria for

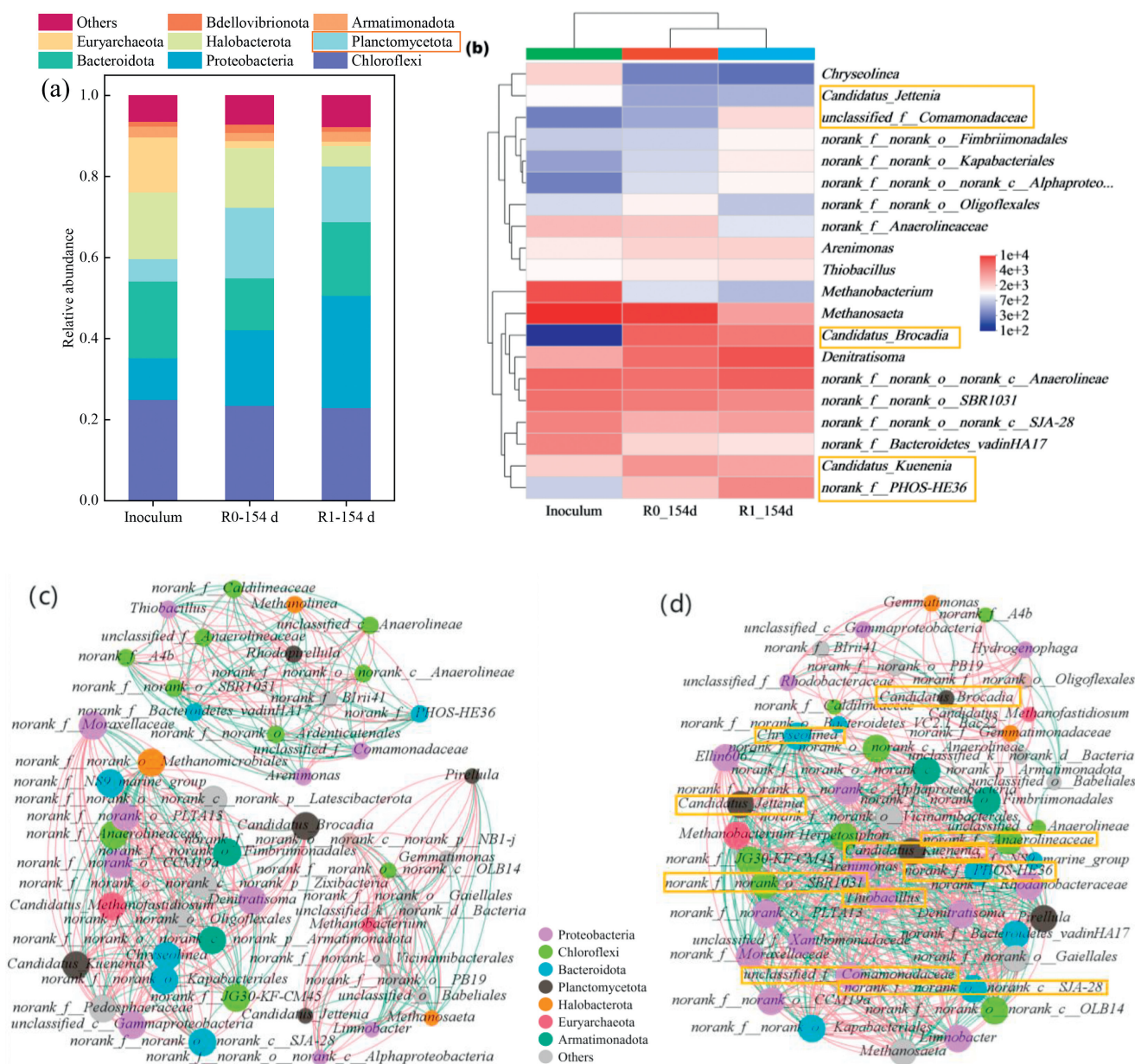


Fig. 3. (a) Relative abundance of the microbial community at the phylum level, (b) relative abundance at the genus level shown as a heat map. Network analysis of the microbial community in the (c) R₀ sludge at 154 d and (d) R₁ sludge at 154 d.

carbon sources, and their increased presence further explains the intrinsic reason for the high denitrification rate achieved in the reactors. The genus *Norank-f-PHOS-HE36* (*PHOS-HE36*) can achieve DNRA [46], and by the end of the culture, its abundance in R₁ was higher than in R₀ (6.45% and 3.24%, respectively), indicating that the addition of Fe(II) had promoted DNRA activity within the Anammox system. This had improved the removal of nitrate produced by Anammox, which in turn improved TN removal. In addition, nitrate-dependent Fe(II) oxidation (NDFO) can be performed by *Unclassified_f_Comamonadaceae* (*Comamonadaceae*), which was present in R₁ at 2.43% [47]. Its activity can reduce NO₂⁻-N to NO₂⁻-N or N₂ and this further improved TN removal. In summary, it is speculated that a Fe(II)/Fe(III) cycle may have occurred in R₁, which improved the efficiency of electron transfer, increased the species diversity and promoted efficient coupling among the nitrogen-removing microorganisms, to improve the nitrogen removal efficiency of the system.

Microbial interactions in the communities of the R₀ and R₁ sludge were explored for Spearman correlation coefficients ≥ 0.5 and *P*-values ≤ 0.05 and these were shown in a network plot (Figs. 3c and d). A total of 49 nodes and 562 edges were identified in R₁ while R₀ contained 50 nodes and 406 edges. The higher number of edges in R₁ indicated that the addition of Fe(II) had improved the network structure among the present microorganisms in R₁. This resulted in a more complex network structure that was beneficial to the system's ability to resist adverse factors and maintain stable nitrogen removal performance [48]. The average degree of the R₁ network was 22.94, which was higher than R₀ (16.24), indicating that the addition of R₁ Fe(II) had facilitated the intercommunication between microorganisms in the system [49].

The nodes in both network plots mainly involved Proteobacteria (R₀: 20%, R₁: 30.61%), Chloroflexi (R₀: 20%, R₁: 18.37%), Bacteroidota (R₀: 12%, R₁: 14.29%), and Planctomycetota (R₀: 10%, R₁: 8.16%). The proportion of network nodes was highly sim-

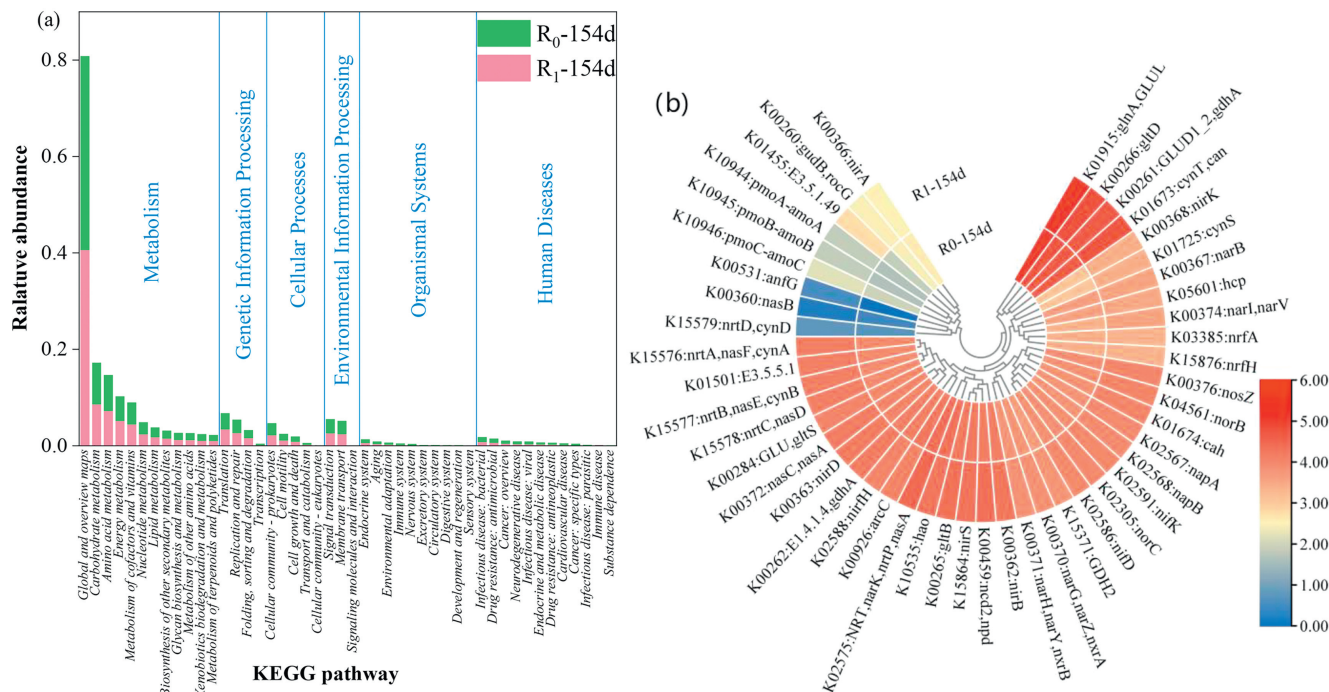


Fig. 4. (a) Predicted abundance of genes assigned to KEGG pathways. (b) Copy number of KO genes related to nitrogen metabolism.

ilar to the relative abundance of these phyla, again indicating that Proteobacteria and Bacterioidota played key roles in Anammox of R_0 and R_1 . The negative correlation among microorganisms in R_1 (45.37% of the total) was higher than in R_0 (41.63%), probably because in R_1 there was more competition for multiple nitrogen removal reactions such as DNRA, NDFO, Feammox. Specifically, *PHOS-HE36*, *Denitratisoma*, *Thiobacillus*, *Comamonadaceae*, and *norank-f-norank-o-norank-c-SJA-28* competed with AAOB for NH_4^+-N , NO_2^--N , and NO_3^--N , further confirming that the presence of multiple nitrogen removal reactions was coupled in R_1 and this was responsible for its high TN removal. The presence of Planctomycetota (*Candidatus_Kueningia*, *Candidatus_Brocadia*, and *Candidatus_Jettenia*) in R_1 was significantly positively correlated with the genera *norank_f_norank_o_Anaerolineaceae*, *norank_f_norank_o_SBR1031* (*SBR1031*) and *Chryseolinea*, microorganisms that have a cleaning role in the system and degrade dead cells while producing volatile organic acids (VFAs) [10]. These VFAs can be used by AAOB, thereby promoting their growth, which explains the positive correlation. In addition, *SBR1031* is involved in sludge aggregation [50]. Overall, the addition of Fe(II) in R_1 enhanced the interspecies interaction within the community, resulting in a higher stability and a stronger nitrogen removal performance than R_0 .

PICRUSt was used for the prediction of microbial community functions, resulting in a total of 6 primary metabolic pathways that were predicted to be present, containing 46 secondary metabolic pathways. The differences in metabolic pathways thus identified between the used sludge of R_0 and R_1 were not significant, and the fraction of metabolism-related pathways reached 76% in both. The highest abundance was observed for amino acid metabolism and carbohydrate metabolism pathways, followed by energy metabolism and cofactor vitamin metabolism, indicators of an active microbial community [51]. Notably, membrane transport and signaling pathways associated with environmental information processing were also detected, suggesting an active exchange of substances took place that may be responsible for synergistic nitrogen removal by AAOB with other heterotrophic bacteria [52]. Specifically, heterotrophic bacteria degrade the EPS that is secreted

by AAOB, as a source of amino acids, while in turn heterotrophic bacteria secrete secondary metabolites such as folic acid that are used by AAOB [53]. This confirms that the Anammox system represents a collaborative community in which nitrogen removal is accomplished by multiple bacterial groups, which is consistent with the results of the microbial communities presented above.

The functional genes predicted to be present in the microbes of the used sludge were predicted by inference using KO. The relative abundance of detected KEGG pathways is summarized in Fig. 4a. We identified 47 predicted functional genes involved in nitrogen metabolism and 68 total KO for nitrogen metabolism, mainly with roles in Anammox, denitrification, and assimilated and dissimilated NO_3^--N reduction. This included genes encoding *NirS* and *Hao* that are involved in AAOB metabolism; *NirS* is a key regulator for the completion of the Anammox process in AAOB [54], and it was predicted to be more abundant in R_1 sludge than in R_0 , further indicating that the addition of Fe(II) facilitated the Anammox reaction. Fig. 4b shows the predicted copy number of genes related to nitrogen metabolism. Compared to R_0 , the predicted abundance of genes associated with denitrification (*norBC*, *nosZ*, *nirDKS*) and assimilated and dissimilated NO_3^--N reduction (*nasAC*, *napAB*, *narGHI*) was higher in R_1 , consistent with the superior nitrogen removal efficacy of R_1 , again explaining at metabolic and genetic levels the intrinsic reasons for the high TN removal rate in R_1 .

All obtained results were combined in a scheme describing the internal metabolic mechanisms that explained how Fe(II) addition in R_1 had contributed to improved nitrogen removal (Fig. 5). The reduced initiation time of R_1 to 55 days and its improved TN removal compared to R_0 was attributed to a combination of the following factors: (1) The addition of Fe(II) to the Anammox system to couple multiple denitrogenation reactions in the system. The details are as follows: the Anammox key functional genes such as *nirS* and *hao*, with high abundance in R_1 and regulated the activity of organisms like *Candidatus-Brocadia*, *Candidatus-Kueningia*, and *Candidatus-Jettenia*, three typical AAOB that perform the Anammox reaction to oxidize NH_4^+-N and NO_2^--N to NO_3^--N and N_2 . The product of Anammox, NO_3^--N , can be converted to NO_2^--N and NH_4^+-N by *nasAC*, *napAB*, *narGHI* regulated microorganisms that

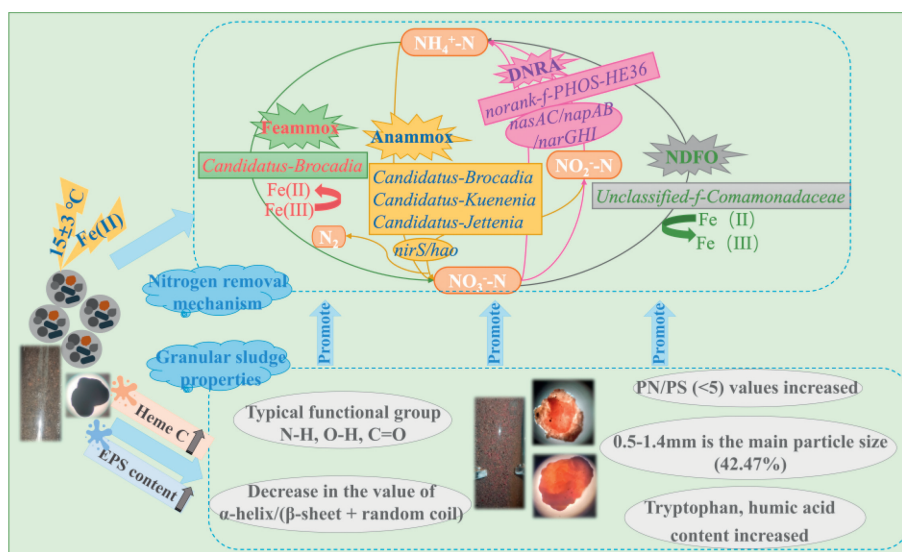


Fig. 5. Schematic of the metabolic mechanisms explaining the experimental observations.

can perform DNRA process (*PHOS-HE36*, etc.) to provide substrate for AAOB and promote its growth and metabolism; it can also be converted by iron-oxidizing bacteria (IOB) (e.g., *Comamonadaceae*) via NDFO process to $\text{NH}_4^+\text{-N}$, which is ultimately removed by the Anammox; and it can be converted by conventional denitrification to N_2 for discharge to the atmosphere. In addition, Fe(II) stimulates *Candidatus-Brocadia* and other iron-reducing bacteria (IRB) to perform Feammox to improve the removal of $\text{NH}_4^+\text{-N}$ in the system. (2) The characteristics of the granular sludge present in the reactor were improved (granule size, granular stability) as a result of the Fe(II) addition, and this also improved the nitrogen removal performance. The amount of EPS produced had increased and its composition had improved, with an increased tryptophan content, improved PN/PS ratio, and more abundant functional groups such as N–H, O–H, and C=O that enhanced the hydrophobicity and improved aggregation of the granular sludge.

These factors in combination ensured efficient and stable microbial nitrogen removal from the system while the reactor was operated at low temperature ($15 \pm 3^\circ\text{C}$).

In this study, the addition of Fe(II) to an Anammox reactor system (R_1) operated at $15 \pm 3^\circ\text{C}$ reduced the initiation time by 10 days and improved TN removal to 89%, compared to 75% in the R_0 that had not received additional Fe(II). The improved efficiency of R_1 was accompanied by a higher SAA and heme c content in the sludge, which improved the activity of AAOB. The addition of Fe(II) promoted the coupled denitrification of Anammox, DNRA, NDFO, and Feammox in R_1 . It further improved the aggregation and stability of the formed granular sludge, which was related to the more abundant presence of N–H, O–H, and C=O functional groups, an increased tryptophan content, and an increased PN/PS ratio of the formed EPS. This increased the fraction of the particles sized 0.5–1.4 mm in the sludge R_1 , resulting in improved sludge stability and better denitrification performance of the Anammox reaction compared to R_0 . The stability of the system was demonstrated by short-term low temperature ($2\text{--}7^\circ\text{C}$) starvation, from which the bacterial community in R_1 recovered faster than that of R_0 . Overall, we conclude that the addition of Fe(II) is beneficial for an Anammox system operated at low temperature.

Declaration of competing interest

The authors declare that they have no known competing financial interests or personal relationships that could have appeared to influence the work reported in this paper.

Acknowledgments

This work was supported by the State Key Laboratory of Geohazard Prevention and Geoenvironment Protection Foundation (No. SKLGP2022Z012) and the National Natural Science Foundation of China (No. 41502333).

Supplementary materials

Supplementary material associated with this article can be found, in the online version, at doi:10.1016/j.ccl.2023.109243.

References

- [1] F. Feng, Z. Liu, X. Tang, et al., *Water Res.* 229 (2023) 119393.
- [2] L. Sindhu, K. Niu, X. Liu, S. Ni, X. Fang, *J. Water Process. Eng.* 43 (2021) 102251.
- [3] M. Zhang, S. Wang, B. Ji, Y. Liu, *Sci. Total Environ.* 692 (2019) 393–401.
- [4] Q. Zhang, J.G. Lin, Z. Kong, Y. Zhang, *Sci. Total Environ.* 833 (2022) 155074.
- [5] D.J.I. Gustavsson, C. Suarez, B.M. Wilen, M. Hermansson, F. Persson, *Sci. Total Environ.* 714 (2020) 136342.
- [6] P. Wu, Y. Chen, X. Ji, et al., *Bioresour. Technol.* 267 (2018) 696–703.
- [7] H. Ma, Y. Zhang, Y. Xue, Y. Zhang, Y. Li, *Sci. Total Environ.* 659 (2019) 568–577.
- [8] S. Wang, H. Yu, J. Zuo, *Environ. Sci.* 41 (2020) 5082–5088.
- [9] J. Dosta, I. Fernandez, J.R. Vazquez-Padin, et al., *J. Hazard. Mater.* 154 (2008) 688–693.
- [10] L. Peng, R. Shi, Y. Tao, et al., *J. Environ. Manag.* 325 (2023) 116542.
- [11] J. Ding, W. Seow, J. Zhou, et al., *Front. Environ. Sci. Eng.* 15 (2021) 7.
- [12] S. Qiao, Z. Bi, J. Zhou, Y. Cheng, J. Zhang, *Bioresour. Technol.* 142 (2013) 490–497.
- [13] Y. Chen, F. Jia, Y. Liu, et al., *Chemosphere* 285 (2021) 131322.
- [14] W. Sun, Q. Banihani, R. Sierra-Alvarez, J.A. Field, *Chemosphere* 84 (2011) 1262–1269.
- [15] W. Liu, T. Li, J. Wang, et al., *Chemosphere* 307 (2022) 136151.
- [16] C. Tang, P. Zheng, C. Wang, et al., *Water Res.* 45 (2011) 135–144.
- [17] S. Sawayama, *J. Biosci. Bioeng.* 101 (2006) 70–72.
- [18] X. Zhang, Z. Chen, Y. Zhou, et al., *Sci. Total Environ.* 648 (2019) 798–804.
- [19] B. Xing, Q. Guo, X. Jiang, et al., *Chem. Eng. J.* 287 (2016) 575–584.
- [20] B. Wang, D. Wu, G.A. Ekama, et al., *Water Res.* 122 (2017) 481–491.
- [21] B. Wang, D. Wu, X. Zhang, et al., *Appl. Microbiol. Biotechnol.* 102 (2018) 6383–6392.
- [22] H. Lu, P. Zheng, Q. Ji, et al., *Bioresour. Technol.* 123 (2012) 312–317.
- [23] W. Chen, S. Chen, F. Hu, et al., *Environ. Sci. Pollut. Res.* 27 (2020) 18661–18671.
- [24] W. Wang, Y. Yan, Y. Zhao, Q. Shi, Y. Wang, *Water Res.* 169 (2020) 115223.
- [25] S. Yuan, M. Sun, G. Sheng, et al., *Environ. Sci. Technol.* 45 (2011) 1152–1157.
- [26] C.G. Kumar, H. Joo, J. Choi, Y. Koo, C. Chang, *Enzyme Microb. Technol.* 34 (2004) 673–681.
- [27] F. Jia, Q. Yang, X. Liu, et al., *Environ. Sci. Technol.* 51 (2017) 3260–3268.
- [28] X. Hou, S. Liu, Z. Zhang, *Water Res.* 75 (2015) 51–62.
- [29] W. Chen, P. Westerhoff, J.A. Leenheer, K. Booksh, *Environ. Sci. Technol.* 37 (2003) 5701–5710.
- [30] J.F. Su, C. Cheng, T. Huang, L. Wei, *Mar. Pollut. Bull.* 117 (2017) 88–97.
- [31] M. Biancalana, K. Makabe, S. Yan, S. Koide, *Protein Sci.* 24 (2015) 841–849.
- [32] R. Du, S. Cao, X. Li, J. Wang, Y. Peng, *Bioresour. Technol.* 300 (2020) 122675.

- [33] J.G. Kuenen, *Nat. Rev. Microbiol.* 6 (2008) 320–326.
- [34] F. Jia, Y. Peng, J. Li, X. Li, H. Yao, *Water Environ. Res.* 93 (2021) 2549–2558.
- [35] H. Xue, W. Wang, H. Xie, Y. Wang, *Sci. Total Environ.* 806 (2022) 151325.
- [36] D. Chen, D. Wang, Z. Xiao, H. Wang, K. Yang, *Bioprocess. Biosyst. Eng.* 41 (2018) 449–455.
- [37] J. Wu, S. Cui, Q. Zhang, et al., *Water Process. Eng.* 50 (2022) 103353.
- [38] Y. Liu, Y. Han, T. Guo, et al., *Bioresour. Technol.* 374 (2023) 128782.
- [39] V. Kouba, R. Darmal, D. Vejmelkova, P. Jenicek, J. Bartacek, *Biotechnol. Prog.* 34 (2018) 277–281.
- [40] L. Zhang, Y. Narita, L. Gao, et al., *Water Res.* 125 (2017) 249–258.
- [41] S. Wang, H. Yu, Q. Su, J. Zuo, *Bioresour. Technol.* 341 (2021) 125762.
- [42] Y. Li, S. Wang, J. Zuo, *China Environ. Sci.* 41 (2021) 1172–1180.
- [43] Z. Wang, X. Wang, Y. Sun, et al., *Chem. Eng. J.* 460 (2023) 141768.
- [44] M. Ali, D.R. Shaw, L. Zhang, et al., *Water Res.* 143 (2018) 10–18.
- [45] X.H. Yi, J. Wan, Y. Ma, Y. Wang, *Biochem. Eng. J.* 107 (2016) 66–74.
- [46] Y. Tao, R. Shi, L. Peng, et al., *Process Saf. Environ. Protect.* 167 (2022) 423–433.
- [47] Y. Yang, C. Xiao, J. Lu, Y. Zhang, *Water Res.* 172 (2020) 115528.
- [48] J. Zhou, Y. Deng, F. Luo, et al., *mBio* 1 (2010) 00169–10.
- [49] T. Ya, S. Du, Z. Li, et al., *Water Res.* 188 (2021) 116540.
- [50] K. Wan, Y. Yu, J. Hu, et al., *Bioresour. Technol.* 357 (2022) 127351.
- [51] B. Yan, J. Fu, S. Xia, et al., *Environ. Sci.* 42 (2021) 3875–3885.
- [52] Y. Li, L. Yao, Q. Sui, et al., *Acta Sci. Circumstantiae* 41 (2021) 92–101.
- [53] Y. Zhao, S. Liu, B. Jiang, et al., *Environ. Sci. Technol.* 52 (2018) 11285–11296.
- [54] M. Strous, E. Pelletier, S. Mangenot, T. Rattei, A. Lehner, *Nature* 440 (2006) 790–794.